IMPROVEMENTS OF CONDENSATION HEAT TRANSFER MODELS IN MARS CODE FOR LAMINAR FLOW IN PRESENCE OF NON-CONDENSABLE GAS

YOUNG-SUK BANG, JI-HAN CHUN[1*], BUB-DONG CHUNG[2] and GOON-CHERL PARK
Nuclear Engineering Department, Seoul National Univ.
[1] BK21 Research Division of SNU for Energy Resource, Seoul National Univ.
[2] Thermal Hydraulic Safety Research Department, Korea Atomic Energy Research Institute
*Corresponding author. E-mail : jhchun@snu.ac.kr

Received January 30, 2009
Accepted for Publication April 27, 2009

The presence of a non-condensable gas can considerably reduce the level of condensation heat transfer. The non-condensable gas effect is a primary concern in some passive systems used in advanced design concepts, such as the Passive Residual Heat Removal System (PRHRS) of the System-integrated Modular Advanced ReacTor (SMART) and the Passive Containment Cooling System (PCCS) of the Simplified Boiling Water Reactor (SBWR). This study examined the capability of the Multi-dimensional Analysis of Reactor Safety (MARS) code to predict condensation heat transfer in a vertical tube containing a non-condensable gas. Five experiments were simulated to evaluate the MARS code. The results of the simulations showed that the MARS code overestimated the condensation heat transfer coefficient compared to the experimental data. In particular, in small-diameter cases, the MARS predictions showed significant differences from the measured data, and the condensation heat transfer coefficient behavior along the tube did not match the experimental data. A new method for calculating condensation heat transfer coefficient was incorporated in MARS that considers the interfacial shear stress as well as flow condition determination criterion. The predictions were improved by using the new condensation model.

KEYWORDS : Condensation Heat Transfer, MARS

1. INTRODUCTION

Even a small amount of non-condensable gas can significantly reduce the level of heat transfer. When condensation occurs at the interface of a liquid film on the wall of a vertical tube, a non-condensable gas will accumulate and form a non-condensable gas layer. This increases the non-condensable gas concentration at the interface between the liquid film and gas, which in turn reduces the condensation heat transfer rate.

Condensation heat transfer is a primary concern in passive systems used in advanced plants to increase the inherent safety [1]. The Passive Secondary Condensing System (PSCS), the Passive Containment Cooling System (PCCS), the Isolation Condensation System (ICS) and the Safety Condenser (SACO) have been adopted as decay heat removal systems in passive reactors, such as the CARR PASSIVE-1300MWe (CP-1300) and the Simplified Boiling Water Reactor (SBWR). The System-integrated Modular Advanced ReacTor (SMART) also uses a passive system, the Passive Residual Heat Removal System (PRHRS). In these systems, condensation heat transfer in vertical tubes is the main heat transfer mechanism, and non-condensable gases can be present. A lower condensation heat transfer rate causes the performance of the heat exchanger to deteriorate, which affects the heat removal capacity in accident conditions and impacts plant safety. It can be also important in a Pressurized Water Reactor (PWR). For example, in a Small Break Loss Of Coolant Accident (SBLOCA), the steam produced in the core can condense in the steam generator tubes through the secondary system cooling. The heat transfer rate in this situation can alter the accident progression and cause reflux condensation and re-criticality.

Many condensation experiments have been performed using a vertical geometry with a variety of fluids [1]. Badger et al. (1930), Meinsenburg et al. (1935), Ullock and Badger (1937) and Shea and Krase (1940) performed condensation experiments in a vertical tubular type condenser. They reported the averaged heat transfer coefficients from laminar to turbulent flow regimes. Carpenter (1948) and Goodykoontz and Dorsch (1966) carried out condensation experiments in a vertical tube at high steam flow rate to determine the local condensation heat transfer coefficients

in a vertical tube. They measured the local axial coolant temperatures and calculated the local condensation heat transfer coefficients. Recently, several studies have been conducted. Siddique (1992) [2] and Kuhn (1995) [3] performed experimental and theoretical studies to determine the effects of non-condensable gases on steam condensation in a vertical tube under forced convection conditions. These studies were aimed at predicting the steam condensation rate in the presence of air or hydrogen in order to analyze the performance of the Isolation Condenser (IC) of the proposed SBWR. Park (1999) [4] also carried out a set of condensation experiments in a vertical tube to test the performance of PCCS in CP-1300. Quite recently, Lee (2007) [5] examined the local condensation heat transfer coefficients in the presence of a non-condensable gas inside a vertical tube simulating the PRHRS of SMART.

The Multi-dimensional Analysis of Reactor Safety (MARS) code was developed by the Korea Advanced Energy Research Institute (KAERI) with the objective of producing a state-of-art realistic thermal hydraulic systems analysis code with multi-dimensional analysis capability [6]. The MARS code is being used in many key areas of the nuclear industry, including PWR safety analysis and accident simulation. However, there are still uncertainties about some heat transfer correlations used by MARS. In particular, there is no reliable model for the condensation phenomena in a vertical tube with a non-condensable gas. In order to utilize the MARS code not only for accident simulation of operating NPPs but also for the design and simulation of advanced reactors, the capability and the applicability of the MARS code should be verified. This can be achieved by simulating various kinds of experiments and comparing the MARS predictions to the experimental data.

In this study, the capability and applicability of the MARS code for predicting the condensation heat transfer for laminar flow in a vertical tube with a non-condensable gas were conducted. Five experiments performed by Goodykoontz [7], Siddique [2], Kuhn [3], Park [4], and Lee [5] were simulated using MARS and those experimental data were compared to the MARS predictions. The differences observed in comparisons were investigated and some improvements for MARS models were suggested.

2. ASSESSMENT FOR CONDENSATION MODEL OF ORIGINAL MARS

2.1 Condensation Heat Transfer Model in Vertical Tube

The Colburn-Hougen diffusion method is used to solve for the liquid/gas interface temperature in the presence of non-condensable gases. The Colburn-Hougen diffusion calculation involves an iterative process to solve for the temperature at the interface between the steam and the water film. The formulation is based on the principle that the amount of heat transferred by condensing vapor to the liquid-vapor interface by diffusing through the non-condensable gas film is equal to the heat transferred through the condensate. From this energy conservation principle, the interface pressure and temperature will be determined by iteration. The heat transfer rate then will be known [8].

The heat flux due to condensation of vapor mass flux, jv, flowing toward the liquid-vapor interface is

$$q_v'' = j_v \cdot h_{fgb} = h_m h_{fgb} \rho_{vb} \ln\left(\frac{1-\frac{P_{vi}}{P}}{1-\frac{P_{vb}}{P}}\right) \quad (1)$$

The heat flux from the liquid film to the wall is calculated by

$$q_l'' = h_c(T_{vi} - T_w) \quad (1)$$

The condensation heat transfer coefficient, h_c, is calculated using the Nusselt Model (1916) and the Shah Model (1979) for laminar flow and for turbulent flow, respectively. The maximum value of two correlations was taken as a final condensation heat transfer coefficient.

The Nusselt expression for vertical surfaces uses the film thickness, δ, as the key parameter.

$$h_{Nusselt} = \frac{k_f}{\delta} \quad (3)$$

Film thickness:

$$\delta = \left(\frac{3\mu_f \Gamma}{g\rho_f \Delta\rho}\right)^{1/3} = \left(\frac{3\mu_f^2 \mathrm{Re}_f}{4g\rho_f \Delta\rho}\right)^{1/3} = 0.9086\left(\frac{\mu_f^2 \mathrm{Re}_f}{g\rho_f \Delta\rho}\right)^{1/3} \quad (4)$$

The Shah's correlation is given by

$$h_{Shah} = h_{sf}\left(1+\frac{3.8}{Z^{0.95}}\right) \quad (5)$$

where,

$$Z = \left(\frac{1}{X}-1\right)^{0.8} P_{red}^{\ 0.4} \quad (6)$$

$$, h_{sf} = h_f(1-X)^{0.8}, \quad (7)$$

Dittus-Boelter coefficient assuming that all fluid is liquid :

$$h_l = 0.023\left(\frac{k_l}{D_h}\right)\mathrm{Re}_l^{0.8}\,\mathrm{Pr}_l^{0.4} \tag{8}$$

where the Reynolds number is given by

$$\mathrm{Re}_l = G_{total}\frac{D_h}{\mu_f} \tag{9}$$

Initially, the liquid-vapor interface partial pressure is assumed as the saturation pressure based on the wall temperature and so, the corresponding T_{vi} is known, and the energy balance equation can be checked by

$$q_l'' = q_v'' \text{ or } h_c(T_{vi} - T_w) = h_m h_{fgb}\rho_{vb}\ln\left(\frac{1-\frac{P_{vi}}{P}}{1-\frac{P_{vb}}{P}}\right) \tag{10}$$

The calculation is iterated until the convergence criterion is met. Total heat flux is calculated by

$$q_{total}'' = h_c(T_w - T_{sppb}) \tag{11}$$

Because MARS is a two-fluid code, the liquid and the gas can both theoretically exchange energy with the wall. Although film condensation is the only condensation mode considered, currently MARS allows a heat flux both to liquid and to gas. The heat flux to liquid is

$$q_f'' = h_c(T_w - T_f) \tag{12}$$

The gas to wall heat flux is the difference between the total heat flux and the liquid to wall heat flux, i.e

$$q_g'' = h_{gas}(T_w - T_{sppb}) \tag{13}$$

Total heat transfer coefficient is calculated by

$$h_{total} = h_c + h_{gas} \tag{14}$$

2.2 Condensation Experiment Modeling by MARS code

Several experimental studies have been performed to examine condensation in the presence of a non-condensable gas in a vertical tube. The research background has been used to support the design of a passive system. In order to evaluate the capability of the MARS code to predict heat transfer of steam and non-condensable gas mixtures in vertical tubes, five experiments were selected and analyzed.

Table 1. Condensation Experiments in a Vertical Tube with Non-condensable Gases

	Goodykoontz (1964)	Siddique (1993)	Kuhn (1997)	Park (1999)	Lee (2008)
	NASA	MIT	UCB	KAIST	POSTECH
Tube length (m)	2.15	2.54	2.4	2.4	2.8
Tube ID (mm)	15.875	46	47.5	47.5	13
Tube Thickness (mm)	1.58	2.4	1.65	1.65	2.5
Secondary jacket ID (mm)	50.8	62.7	76.2	100	40
Non-condensable gas	-	air, helium	air, helium	air	nitrogen
Secondary cooling	Forced Convection	Forced Convection	Forced Convection	Forced Convection	Forced Convection
Steam flow (g/s)	4.2-14.7	2.4-8.9	8.2-17	2-11	1.8-7.8
Inlet air mass fraction (%)	-	10-35	0-40	10-70	0-40
Pressure (MPa)	0.1	0.1-0.5	0.1-0.5	0.17-0.5	0.1-0.13
HTC (W/m^2K)	4485-11867	100-25000	500-13000	100-7000	300-27900

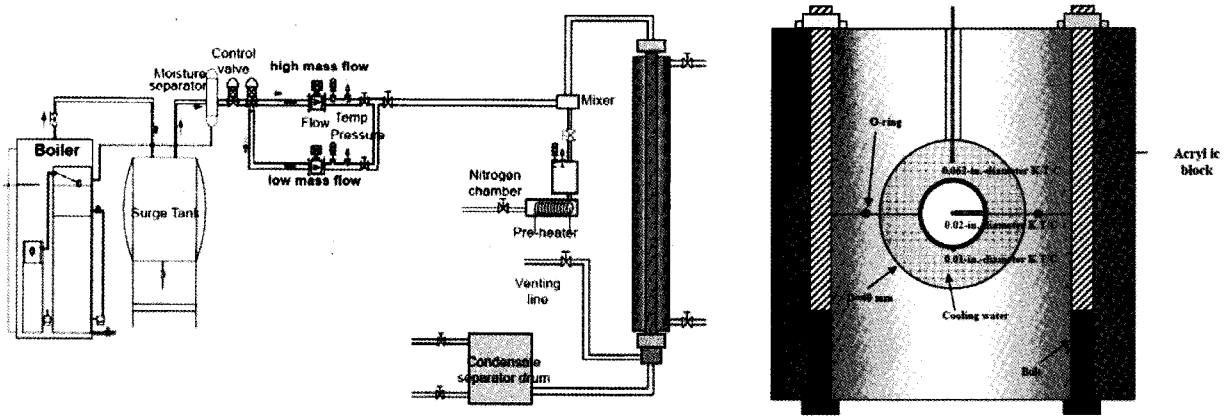

Fig. 1. Lee's Experimental Apparatus

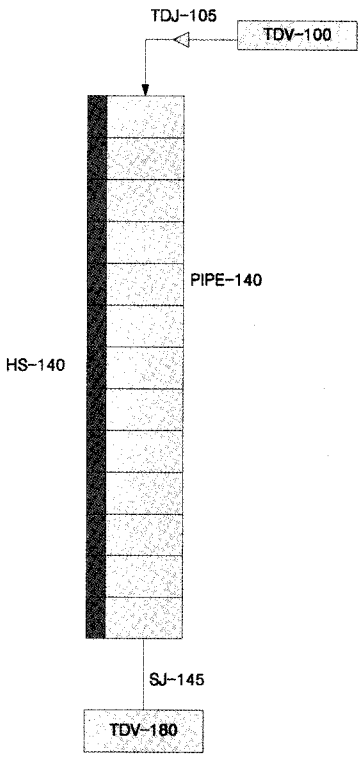

Fig. 2. MARS Nodalization Scheme for the Condensation Experiment Facility

Table 1 summarizes the experiments analyzed. All had a similar test section geometry and secondary cooling. As a representative, Fig. 1 shows a schematic diagram of the Lee's experimental apparatus. The experimental facilities consisted of a steam generator, a non-condensable gas mixing system, a test section with a condensing tube and its surrounding coolant jacket, a lower plenum, venting and draining systems, and a unit for a data acquisition system. The test section consisted of an inner condenser tube and an outer cooling jacket. The vapor and non-condensable gas mixture was injected into the top of the vertical condensing tube and cooling water was injected into the bottom of the cooling jacket placed outside the condensing tube. The injected gas mixture was cooled and condensed by heat transfer through the condensing tube wall. At different axial locations, thermocouples were welded: to the outer surface of the condensing tube to measure the outer surface temperature, through the condensing tube to measure the mixture bulk temperatures, and to the outer side of the coolant jacket to measure the coolant temperatures.

Fig. 2 shows the MARS code nodalization scheme for the condensation experiments. The MARS nodalization used for this simulation contained the following components: pipe, annulus, time dependent volume and junction, and heat structure. Pipe component, PIPE-140, was used to model the condenser tube. The time-dependent volumes acting as infinite mass and energy sources or sinks were used to represent the boundary conditions for steam and non-condensable gas flow inside the condensing tube. The time-dependent volume, TDV-100, was used to provide the inlet flow of steam/non-condensable gas mixture. The pressure and temperature of this volume were determined using the measured bulk inlet pressure and temperature. The inlet steam was saturated. Therefore, the partial pressure of a non-condensable gas was determined by subtracting the saturated pressure of steam from the bulk inlet pressure after being determined by the inlet temperature. The inlet flow rate of the steam/non-condensable gas mixture was controlled by the time-dependent junction, TDJ-105, and was used in cases in which the experimental data gives the mixture flow rate. When the steam flow rate and non-condensable gas flow rate were given separately,

their sum was simply used as the flow rate at the time-dependent junction, TDJ-105. The time-dependent volume, TDV-180, was used to provide the outlet boundary condition, and this condition was determined using the experimental data.

The heat structure, HS-140, was used to represent the heat transferred from the steam/non-condensable gas mixture to the coolant through the condensing tube. Heat transfer is a process consisting of condensation heat transfer in the condensing tube, conduction in the tube wall, and convective heat transfer in the cooling jacket. The overall heat transfer process is dominated by the part with the largest heat resistance. In the M82 case of Lee's experiment as an example, the heat transfer coefficients of the secondary side, the tube metal, and the inside of the tube wall were calculated to about 4000~5000 W/m^{2}K, 7000~8000 W/m^{2}K, and 20,000 W/m^{2}K, respectively. This means that the heat resistance (1/hA) is largest at the secondary side, second largest at the tube metal, and smallest at the tube inside. In order to examine the condensation heat transfer of the inside of the condensing tube, other parts such as conduction or secondary side cooling must be accurately modeled. It should be emphasized that some of the experiment researchers used a bubble mixing technique to measure bulk temperatures in the cooling jacket. The bubble was utilized to enhance the mixing and eliminate the temperature gradient. However, injected air bubbles can enhance the overall heat transfer and distort the flow pattern. In the early stages of the study, the MARS model included the secondary side. In comparison between the MARS predictions and the measured data, the heat transfer rates of the MARS calculations were much smaller than those in the experimental data. It was concluded that the unexpected enhancement of the heat transfer resulted from the turbulence of the injected mixture and the coolant or the enhanced mixing by the injected bubbles. However, there is no specific model to treat turbulence or mixing in the MARS code, and the amount of heat transfer enhancement and the effects of injected bubbles cannot be identified. Considering all the things above, it was decided not to model the secondary and to directly use the measured outer wall temperatures as a boundary condition, so that the undesirable effects could be removed as much as possible.

2.3 Results of Simulations

Figs. 3-7 compare the experimental data and the MARS calculation results. First of all, the MARS predictions showed different trends from Goodykoontz's and Lee's experimental data. The experimental data of the other experiments and the MARS predictions showed that the HTCs varied inversely and downwardly along the tube. However, the MARS predictions for Goodykoontz's and Lee's data showed that the HTCs decreased almost linearly along the tube. In the current MARS code, the condensation HTC was calculated by both the Nusselt model and the Shah model, and, simply, the larger value was used. In Goodykoontz's experiments and Lee's experiments, the Shah model, which is to be used for turbulent flow, was used just because its HTC was larger than the one found by the Nusselt model although, judging from the film Reynolds number, all the experiment's flow conditions were laminar. After examining the variables in the calculation scheme of the MARS code, the hydraulic diameter was found to

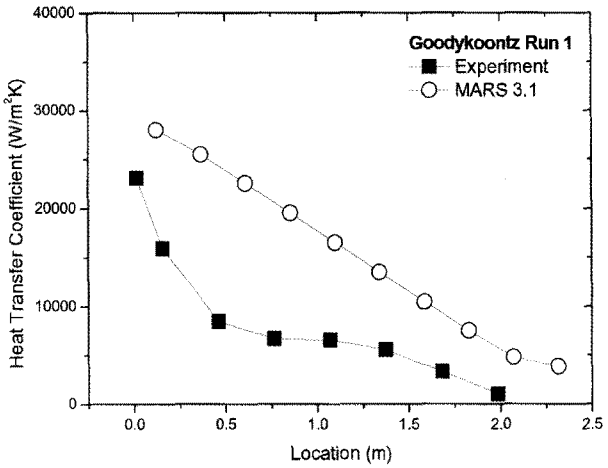

Fig. 3. Comparison of the MARS Predictions with the Experimental Data of Goodykoontz's Experiment (Run 1 Case; inlet Pressure 101.3 kPa, Inlet Temperature 112.2 °C, Inlet Steam Flow Rate 31.3 kg/hr)

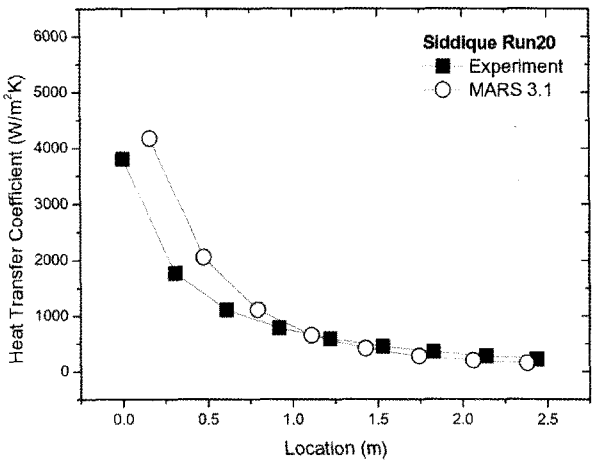

Fig. 4. Comparison of the MARS Predictions with the Experimental Data of Siddique's Experiment (Run 20 Case; Inlet Pressure 119.0 kPa, Inlet Temperature 100.3 °C, Inlet Steam/Non-condensable Gas Mixture Flow Rate 25.0 kg/hr)

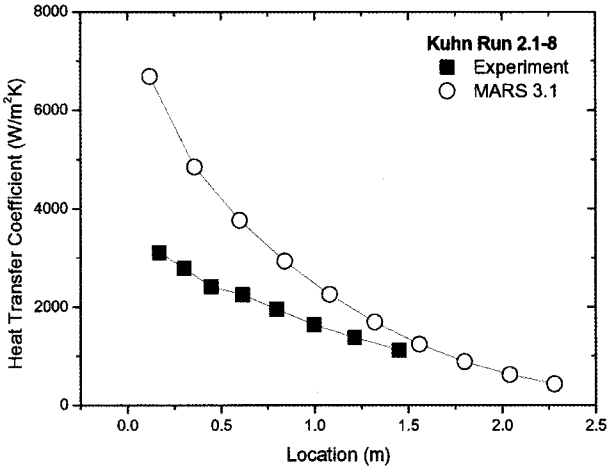

Fig. 5. Comparison of the MARS Predictions with the Experimental Data of Kuhn's Experiment (Run 2.1-8 Case; Inlet Pressure 418.1 kPa, Inlet Temperature 140.7 °C, Inlet Steam/Non-condensable Gas Mixture Flow Rate 58.4 kg/hr)

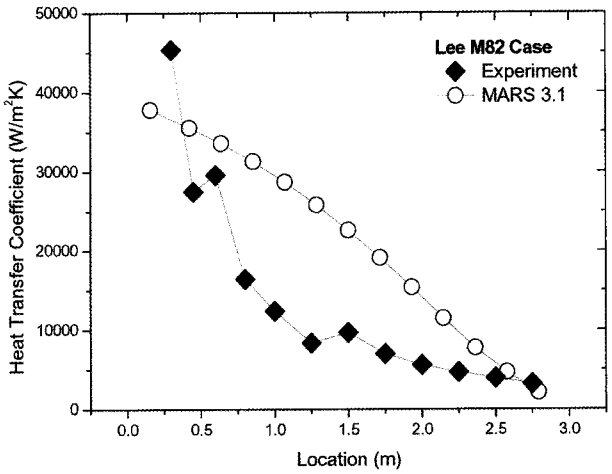

Fig. 7. Comparison of the MARS Predictions with the Experimental Data of Lee's Experiment (M82 Case; Inlet Pressure 131.17 kPa, Inlet Temperature 105.1 °C, Inlet Steam/Non-condensable Gas Mixture Flow Rate 30.1 kg/hr)

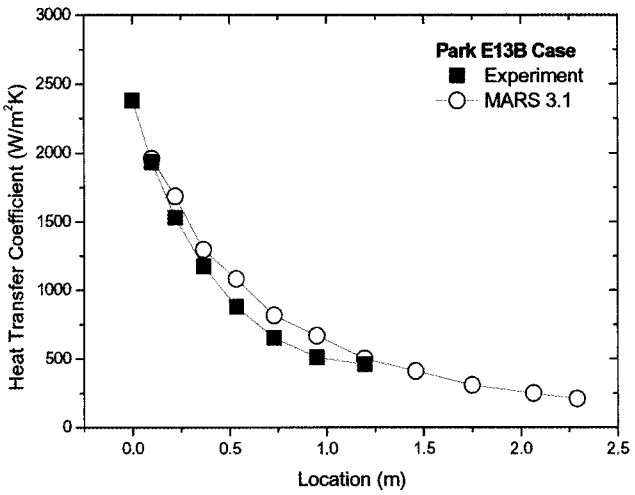

Fig. 6. Comparison of the MARS Predictions with the Experimental Data of Park's Experiment (E13B Case; Inlet Pressure 185.4 kPa, Inlet Temperature 110.5 °C, Inlet Steam/Non-condensable Gas Mixture Flow Rate 27.0 kg/hr)

be the most dominant factor in determining which correlation would be used. In Shah's correlation, the hydraulic diameter D_h is the denominator. It is also related to the G_{total} in which square of D_h is the denominator. Therefore, the heat transfer coefficient h_{shah} increases with decreasing diameter. In other words, using the current MARS criterion, which employs a larger HTC, the correlation for calculating the condensation HTC was chosen not by the film Reynolds number but by the hydraulic diameter. As shown in Table 1, Lee's and GoodyKoontz's experiments use a small diameter condenser tube. In those cases, Shah's correlation, which is not applicable, was used to calculate the condensation HTC. It should be emphasized that the model or correlation must be used in its applicable range. In small diameter cases, it was observed that MARS used a not-applicable correlation. It is obvious that the correlation selection criteria of the current MARS code should be improved.

MARS overestimated the HTC. This is a problem about the accuracy of the correlation itself. The Nusselt model used in the current MARS code has several strict assumptions [8].

1. Fluid properties are constant.
2. Vapor exerts no drag on the liquid surface.
3. Liquid subcooling is neglected.
4. Momentum changes in the laminar liquid annular film are negligible.
5. The heat transfer occurs via conduction through the laminar liquid annular film.

However, these assumptions are not realistic in many practical conditions. MARS predictions for laminar flow can be improved by updating the heat transfer model.

3. IMPROVEMENTS OF CAPABILITY OF MARS FOR PREDICTING CONDENSATION

3.1 Improvement of Correlation Determination Criterion

In the laminar regime, conduction plays the dominant role in heat transfer, and the velocity profile within a liquid

film can be described by a quadratic or cubic function. On the other hand, in the turbulent regime, heat transfer is influenced by turbulent mixing or eddy motion. Therefore, it is important to determine correct flow conditions and to use a proper correlation. The film Reynolds number is widely used as a measure to determine the flow condition: laminar or turbulent [9]. In many studies, several critical Reynolds numbers were suggested ranging from 400 to 3600 [10]. The critical Reynolds number for the transition from laminar to turbulent flow can be 1800, which is the upper limit of the applicable range of Nusselt's correlation [9]. Instead of comparing the calculated heat transfer coefficients, the film Reynolds number was checked and Shah's correlation was used only if it was higher than 1800.

3.2 Improvement of Condensation Heat Transfer Coefficient Correlation

Lee (2008) reported that the interfacial shear stress increases as the condenser tube diameter decreases for the same mixture Reynolds number [5]. The condensation heat transfer coefficients also increase due to the shear stress. The effect of the interfacial shear stress was not sufficiently considered in previous correlations using the Reynolds number. For example, the accuracy of the correlations of Vierow and Schrock (1991) [11] and of Kuhn (1997) [3] varied considerably with the condenser tube diameter due to shear stress. Lee developed a new correlation to improve the accuracy of the predictions regardless of the condenser tube diameter. In order to consider the interfacial shear stress, a dimensionless shear stress was used to develop a new correlation. On account of its simplicity, the degradation factor method was used to correlate the present data.

The dimensionless shear stress is defined as

$$\tau^*_{mix} = \frac{\tau_{mix}}{g\rho_f L} = \frac{1/2\rho_{mix}u^2_{mix}f}{g\rho_f L} \quad (15)$$

where ,

$$u_{mix} = \frac{\mathrm{Re}_{mix}\,u_{mix}}{\rho_{mix}d_i}, \quad (16)$$

$$L = \left(\frac{\nu_f^2}{g}\right)^{1/3}, \quad (17)$$

$$f = 0.079\,\mathrm{Re}_{mix}^{-1/4} \text{ for } \mathrm{Re}_{mix} > 2{,}300 \text{ or } f = \frac{16}{\mathrm{Re}_{mix}} \text{ for } \mathrm{Re}_{mix} < 2{,}300 \quad (18)$$

The degradation factor is given by

$$f_{pure} = \frac{h_{\exp.pure}}{h_{Nu}} = 0.8247\tau^{*\,0.3124}_{mix} \quad \text{for } 0.06 < \tau^*_{mix} < 46.65 \quad (19)$$

The modified condensation HTC is obtained by multiplying the HTC of the Nusselt model by the degradation factor. The Colburn-Hougen method in the original MARS code was still used to obtain the interface temperature and simulate the condensation heat transfer with non-condensable gas.

3.3 Results of Improved MARS Code

Figs. 8-12 compare the experimental data with the predictions of the modified MARS code. They show that the new method, which considers the shear stress and the new criterion, provided better results than the old method did. In particular, in small diameter cases, such as Goodykoontz's and Lee's experiments, the MARS calculation results were greatly improved.

It is also observed that the HTCs are lower than predicted by the existing MARS code. This is because the heat transfer is enhanced and h_c is increased. It should be clarified that MARS calculates the total heat transfer coefficient through $h_{total} = h_c + h_{gas}$. The heat transfer coefficient for the gas phase, h_{gas}, is determined by

$$h_{gas} = \frac{q''_g}{(T_w - T_{spp})}$$

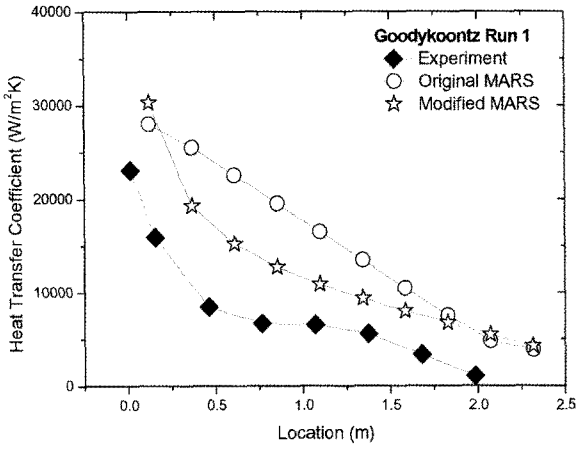

Fig. 8. Comparison of the Original and Modified MARS Predictions with the Experimental Data of Goodykoontz's Experiment (Run 1 case; Inlet Pressure 101.3 kPa, Inlet Temperature 112.2 °C, Inlet Steam Flow Rate 31.3 kg/hr)

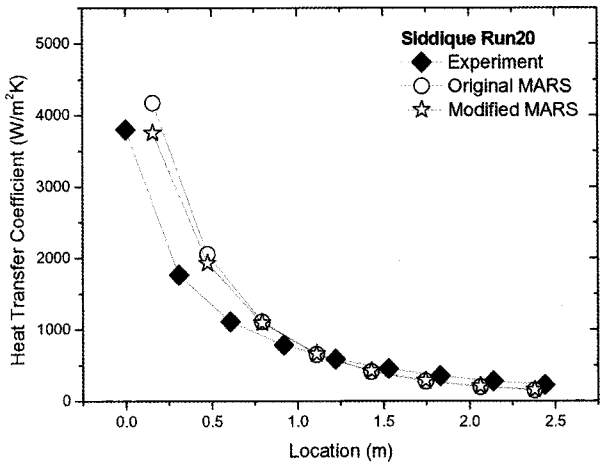

Fig. 9. Comparison of the Original and Modified MARS Predictions with the Experimental Data of Siddique's Experiment (Run 20 Case; Inlet Pressure 119.0 kPa, Inlet Temperature 100.3 °C, Inlet Steam/Non-condensable Gas Mixture Flow Rate 25.0 kg/hr)

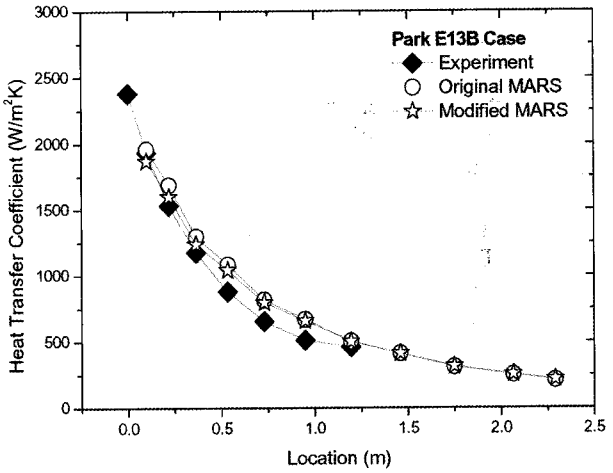

Fig. 11. Comparison of the Original and Modified MARS Predictions with the Experimental Data from Park's Experiment (E13B case; Inlet Pressure 185.4 kPa, Inlet Temperature 110.5 °C, Inlet Steam/Non-condensable Gas Mixture Flow Rate 27.0 kg/hr)

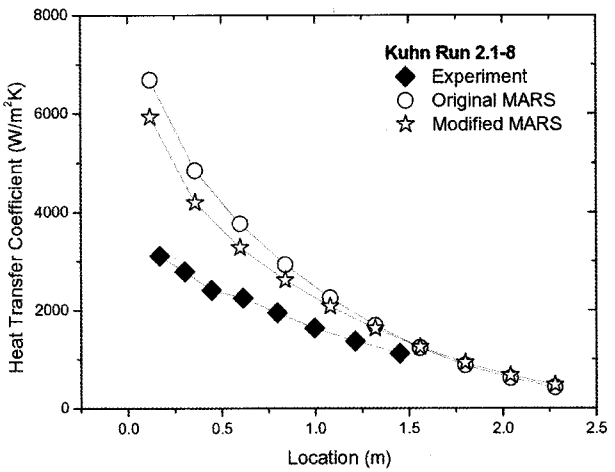

Fig. 10. Comparison of the Original and Modified MARS Predictions with the Experimental Data of Kuhn's Experiment (Run 2.1-8 Case; Inlet Pressure 418.1 kPa, Inlet Temperature 140.7 °C, Inlet Steam/Non-condensable Gas Mixture Flow Rate 58.4 kg/hr)

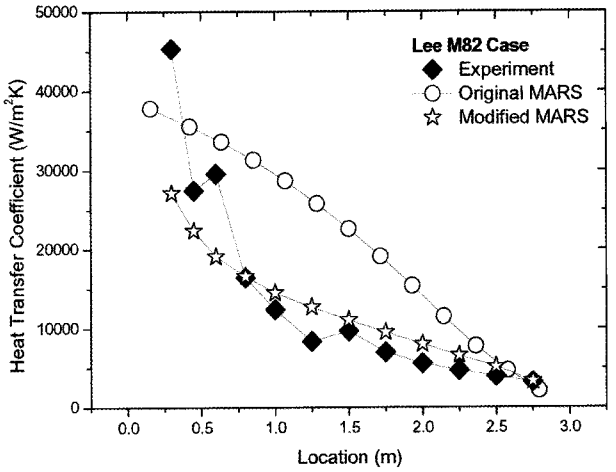

Fig. 12. Comparison of the Original and Modified MARS Predictions with the Experimental Data of Lee's Experiment (M82 Case; Inlet Pressure 131.17 kPa, Inlet Temperature 105.1 °C, Inlet Steam/Non-condensable Gas Mixture Flow Rate 30.1 kg/hr)

while,

$$q_g'' = q'' - q_f'' \quad \text{and} \quad h_c = \frac{q''}{(T_w - T_{spp})} = \frac{q_f''}{(T_w - T_{liq})}$$

T_{spp} = steam saturation partial pressure
T_{liq} = liquid phase temperature.
Rearranging the above equations, the following equation can be obtained.

$$h_c(T_{liq} - T_{spp}) = h_{gas}(T_w - T_{spp})$$

Adopting Lee's correlation, HTCF was increased and T_w was also increased due to enhanced heat transfer. Therefore HTCG was much decreased and total HTC

($h_{total} = h_c + h_{gas}$) was decreased. That is because MARS is a two-fluid code: the liquid and the gas can both theoretically exchange energy with the wall. Although film condensation is the only condensation mode considered, currently MARS allows a heat flux both to liquid and to gas.

To predict the condensation heat transfer coefficient properly is important not only in the PRHRS of SMART but also in operating NPPs. For example, the condensation heat transfer can occur in steam generator tubes that have a small diameter in a certain type of small break LOCA (loss of coolant accident). According to the applied heat transfer model and its accuracy, the prediction of accident progression and consequences can vary considerably.

4. CONCLUSION

This study examined the capability of the MARS code to model condensation heat transfer in a vertical tube with a non-condensable gas. Overall, the current MARS code overestimated the condensation heat transfer coefficient in laminar flow condition. In particular, in small-diameter cases, the heat transfer coefficient trends along the tube did not compare well with the experimental data. This was attributed to inappropriate selection of the correlation and use of the Nusselt's correlation, researchers having had some ideal but unrealistic assumptions.

The condensation heat transfer model was improved by modifying the method to determine the correlation and incorporating the degradation factor developed by Lee to consider interfacial stress in MARS. The modified MARS code predicted improved results of the tube condensation in laminar flow condition.

ACKNOWLEDGEMENTS

This study was performed as part of the Long-and-Mid-term Nuclear R&D Programs funded by the Ministry of Education, Science and Technology of Korea.

NOMENCLATURE

Roman Symbols

- D_h hydraulic diameter (m)
- g gravitational constant (m/s^2)
- h heat transfer coefficient (W/m^2·K)
- h_{fgb} steam minus liquid saturation enthalpy at steam partial pressure in the bulk (W/m^2·K)
- h_l Dittus-Boelter coefficient assuming all fluid is liquid (W/m^2·K)
- h_{sf} superficial heat transfer coefficient (W/m^2·K)
- j mass flux
- k thermal conductivity (W/m·K)
- P_{red} reduced bulk pressure, $P/P_{critical}$
- Pr Prandtl number
- Re Reynolds number
- T_{spp} saturation temperature based on partial pressure (K)
- X static vapor quality = (mass steam + mass noncondensable) / (mass steam + mass noncondensable + mass liquid)

Greek Letters

- Δ change
- δ film thickness (m)
- ρ density (kg/m^3)
- μ dynamic viscosity (Ns/m^2)
- v viscosity (m^2/s)
- Γ liquid mass flow rate per unit periphery (kg/m·s)

Subscripts

- b bulk property
- f fluid phase
- i interface, inner
- l bulk liquid phase
- mix mixture
- v gas phase
- w wall

REFERENCES

[1] Kim, S, J, "Turbulent film condensation of high pressure steam in a vertical tube of passive secondary condensation system", Ph.D. dissertation, Korea Advanced Institute of Science and Technology, Korea, 2000

[2] Siddique, M.S., "The effects of noncondensable gases on steam condensation under forced convection conditions", Ph.D. dissertation, Massachusetts Institute of Technology, 1992

[3] Kuhn, S.Z., "Investigation of heat transfer from condensing steam-gas mixtures and turbulent films flowing downward inside a vertical tube", Ph.D. dissertation, University of California, Berkeley, 1995

[4] Park, H.S., "Steam condensation heat transfer in the presence of noncondensables in a vertical tube of passive containment cooling system", Ph.D. dissertation, Korea Advanced Institute of Science and Technology, Korea, 1999

[5] Lee, K.Y., "The effects of noncondensable gas on steam condensation in a vertical tube of passive residual heat removal system", Ph.D. dissertation, Department of Mechanical Engineering, Pohang University of Science and Technology, Korea, 2007

[6] "MARS code manual volume II: Input Requirements", KAERI/TR-2811/2004, Korea Atomic Energy Research Institute, 2007

[7] Goodykoontz, Jack H. and Dorsch, Robert G., "Local heat transfer coefficients for condensation of steam in vertical downflow within a 5/8-inch-diameter tube", NASA TN D-3326, National Aeronautics and Space Administration, 1966

[8] "MARS code manual volume I: Code Structures, System Models, and Solution Methods", KAERI/TR-2812/2004, Korea Atomic Energy Research Institute, 2007

[9] Frank P.Incropera, David P. DeWitt, "Introduction to Heat Transfer, Second Edition", John Wiley&Sons, Inc., 1993

[10] Kim, K.T., "A semi-empirical heat transfer coefficient for laminar and turbulent film condensation on a vertical surface", Ph.D. dissertation, Korea Advanced Institute of Science and Technology, Korea, 1990

[11] Vieriow, K.M. and Schrock, V.E., Condensation in a natural circulation loop with noncondensable gases: Part I-Heat Transfer, *Proceedings of the International Conference on Multiphase Flow*, pp. 183-186, Tsukuba, Japan, 1991